

Testing biological network motif significance with exponential random graph models

Alex Stivala* Alessandro Lomi*†

December 21, 2024

Abstract

Analysis of the structure of biological networks often uses statistical tests to establish the over-representation of motifs, which are thought to be important building blocks of such networks, related to their biological functions. However, there is disagreement as to the statistical significance of these motifs, and there are potential problems with standard methods for estimating this significance. Exponential random graph models (ERGMs) are a class of statistical model that can overcome some of the shortcomings of commonly used methods for testing the statistical significance of motifs. ERGMs were first introduced into the bioinformatics literature over ten years ago but have had limited application to biological networks, possibly due to the practical difficulty of estimating model parameters. Advances in estimation algorithms now afford analysis of much larger networks in practical time. We illustrate the application of ERGM to both an undirected protein-protein interaction (PPI) network and directed gene regulatory networks. ERGM models indicate over-representation of triangles in the PPI network, and confirm results from previous research as to over-representation of transitive triangles (feed-forward loop) in an *E. coli* and a yeast regulatory network. We also confirm, using ERGMs, previous research showing that under-representation of the cyclic triangle (feedback loop) can be explained as a consequence of other topological features.

Keywords— motifs, biological networks, exponential random graph models, ERGM

1 Introduction

Molecular interactions in biological systems are often represented as networks [1]. Some such networks are inherently undirected, such as protein-protein interaction (PPI) networks [2]. Others may be directed, such as gene regulatory networks, where nodes represent operons, and arcs (directed edges) represent transcriptional interactions between them. Much research with such biological networks has concerned “motifs”, small subgraphs which occur more frequently than would be expected by chance. Motifs have been considered the building blocks of complex networks [3–6]. The biological significance of network motifs derives from their possible interpretation as signs of evolutionary events [7, 8].

Two simple examples of motifs in undirected networks are triangles (three-cycles) and squares (four-cycles) [8]. Directed networks allow for a larger set of potentially important motifs [3, 7, 8], which can be quite complicated, leading to problems of consistency in their definition [9].

It is worth noting that such (three-node) motifs are an idea with a long history in social network analysis, where the counts of all sixteen possible three-node directed graphs (triads) is known as the triad census [10–13]. A systematic naming convention has been developed that is based on the number of mutual, asymmetric, and null (M , A , and N) dyads in the triad, followed by a letter to distinguish the orientation if it is not unique (Fig. 1). For example, the transitive triangle is designated 030T, which distinguishes it from the cyclic triad 030C. Although in common usage in social network research, and cited by Milo *et al.* [3] and Saul & Filkov [14] in the context of biological networks, this naming convention is rarely used in discussions of motifs in the bioinformatics or biology literature. There are efficient algorithms for computing the triad census [15, 16], implemented in widely used general purpose graph libraries such as igraph [17] and NetworkX [18]. The triad census has recently been extended to colored triads, that is, distinguishing the nodes in the triads based on a categorical attribute assigned to them [19]. It has long been noted in the social networks literature that the dyad census constrains the triad census, and yet empirical social networks often still have counts for some triads greater than expected given those constraints [20].

To determine if a motif is over-represented, the count of the motif in an observed network is compared to the distribution of its counts in a set of simulated random networks [6] (it is also possible to determine the significance of motif over-representation without simulation [21, 22]). This leads to the problem of choosing the appropriate random networks (null model), and some

*Institute of Computational Science, Università della Svizzera italiana, Lugano, 6900, Switzerland. Email: alexander.stivala@usi.ch

†The University of Exeter Business School, Exeter, EX4 4PU, United Kingdom

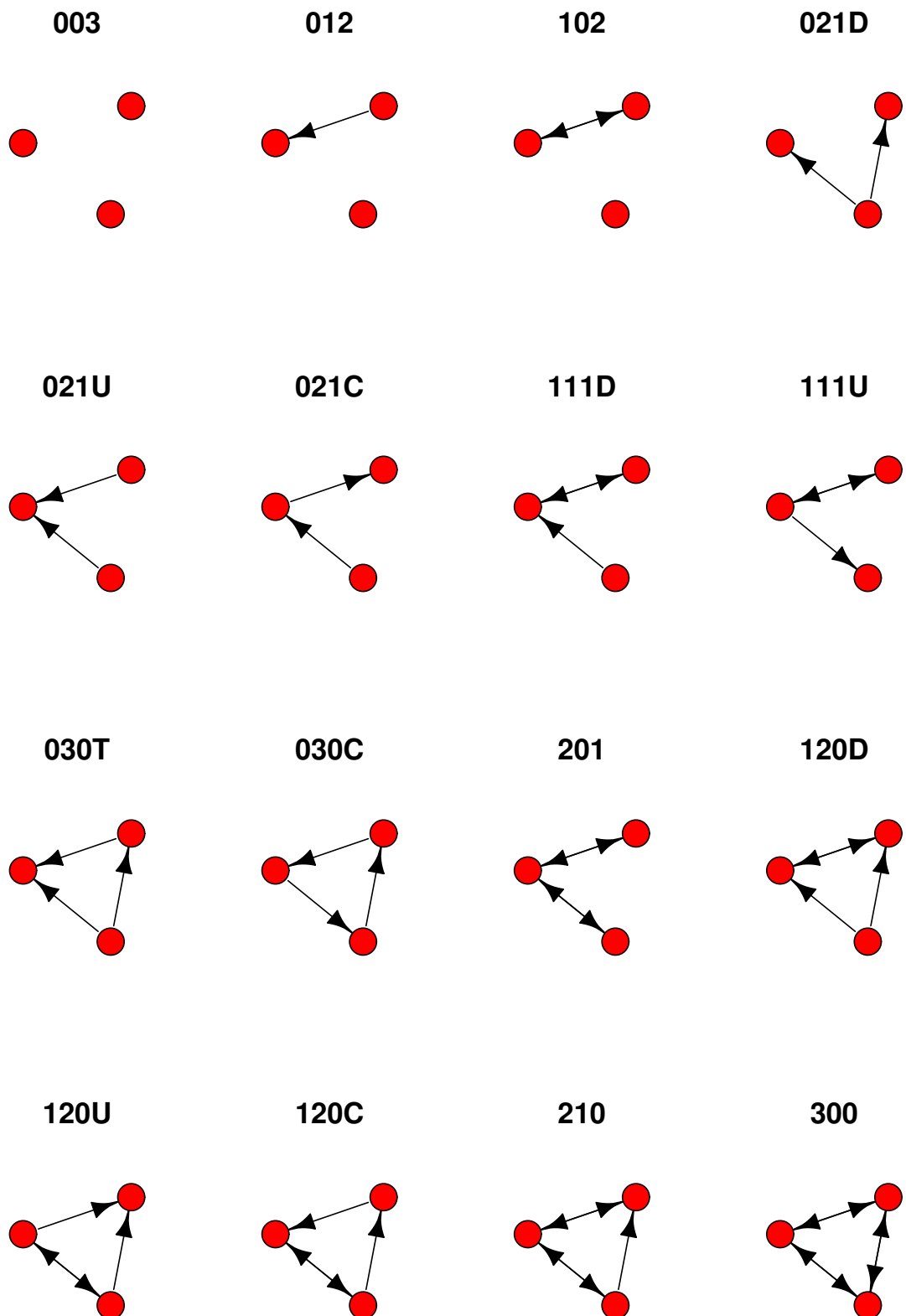


Figure 1: Triad census classes labeled with the MAN (mutual, asymmetric, null) dyad census naming convention. When the dyad census does not uniquely identify a triad, a letter designating “up”, “down”, “transitive”, or “cyclic” is appended.

supposed motifs have been found to not be significantly over-represented, and occur with the observed frequencies simply due to topological properties of random networks [23] or correlations between motifs created by the randomization process [24], although such correlations can also occur even with uniform sampling [25].

Estimating motif (triad census) significance by comparing the triad census of an empirical network to that of ensembles of random graphs also has a long history, for example the conditional uniform graph (CUG) distribution [26–28], conditional on the dyad census (U|MAN) [12], or on the degree distribution [29]. A more modern variation on a similar idea is the dk -series [30, 31], a sequence of nested network distributions of increasing complexity, fitting in turn density, degree distribution, degree homophily, average local clustering, and clustering by degree [31].

The recent work of Fodor *et al.* [25] shows that the assumptions of mainstream methods for motif identification, specifically normally distributed motif frequencies and independence of motifs, do not always hold, and that as a consequence, such methods cannot always correctly estimate the statistical significance of motif over-representation.

Aside from such intrinsic statistical limitations, it may be the case that the apparent statistical over-representation of motifs has no evolutionary or functional significance [32–34], and the choice of null model is a critical factor in this lack of evident relationship between over-representation and evolutionary preservation [32, 35]. Alternatively, the apparent lack of functional significance [34] may be due to too narrow a definition of “function” [36]. Recently, it has also been suggested that elementary motifs are a lower level of structure than that which is most functionally relevant in gene regulatory networks characterizing different physiological states [37].

It might also be the case that particular motifs are over-represented, not because they are evolutionarily selected for function, but because of spatial clustering [38]. For example, in the context of PPI networks, we might expect that interactions would be over-represented between proteins that share a subcellular location, and under-represented between those that do not, since proteins known to interact usually have the same subcellular locations [39]. Indeed PPI networks can be used as predictors of subcellular location [40, 41].

There are many algorithms for motif discovery in complex networks; for a recent review, see Jazayeri & Yang [42], although in the present work we are considering only static, not temporal, networks. Although they differ in many details, especially regarding computational efficiency and scalability, these motif discovery algorithms work fundamentally in the manner described above. That is, they count occurrences of a motif in the observed network, and compare this to the distribution of the motif’s frequency in an ensemble of randomized versions of the original network (typically preserving degree sequence). Therefore these conventional methods all test the significance of one motif at a time, assuming independence of motifs, and are all potentially subject to the problems described by the recent work of Fodor *et al.* [25].

In this work we describe a different approach to determining motif significance in complex networks, which can potentially overcome these problems. Rather than comparing the observed frequency of a candidate motif to its frequency in a set of randomized networks, we take a model-based approach. Specifically, we estimate parameters of a model (an exponential random graph model, abbreviated ERGM) of the observed network. These parameters correspond to substructures which resemble potential motifs of interest. This allows the significance of the candidate motifs to be tested simultaneously in a single model, in such a way that independence of the motifs is not assumed.

We demonstrate this approach in biological networks (both undirected (PPI) and directed gene regulatory networks) using some recently developed ERGM estimation methods [43–46], which allow estimation of models for larger networks that was practical with earlier methods of ERGM parameter estimation.

The remainder of this article is organized as follows. First, we describe ERGMs, and review the literature on the application of ERGMs to biological networks. We then report the biological networks considered in this work, and the details of the ERGM configurations, estimation methods, and goodness-of-fit tests we used. Following that, we present and discuss new ERGM models of these networks, comparing the inferences as to motif significance with existing published results using conventional motif discovery methods. In the next section, we detail the limitations of this application of ERGMs, and indicate some potential future work. We conclude with a summary of the inferences drawn from the ERGM models of the networks considered.

2 Exponential random graph models

ERGMs are widely used in the social sciences, typically to model social networks [47–50]. Cimini *et al.* [51] is a recent review of ERGMs for modeling real-world networks, from a statistical physics viewpoint.

An ERGM is a probability distribution with the form

$$\Pr(X = x) = \frac{1}{\kappa(\theta)} \exp \left(\sum_A \theta_A z_A(x) \right) \quad (1)$$

where

- $X = [X_{ij}]$ is a 0-1 matrix of random tie variables,
- x is a realization of X ,
- A is a “configuration”, a (small) set of nodes and a subset of ties between them,

- $z_A(x)$ is the network statistic for configuration A ,
- θ_A is a model parameter corresponding to configuration A ,
- $\kappa(\theta)$ is a normalizing constant to ensure a proper distribution.

Given an observed network x , we aim to find the parameter vector θ which maximizes the probability of x under the model. Then for each configuration A in the model, its corresponding parameter θ_A and its estimated standard error allow us to make inferences about the over- or under-representation of that configuration in the observed network. If θ_A is significantly different from zero, then if $\theta_A > 0$ the configuration A is over-represented, or under-represented if $\theta_A < 0$.

Note that a “configuration”, unlike a motif (in its most common usage) or the triad census classes, is not an induced subgraph. That is, it does not include every edge in the original graph of which it is a subgraph: a configuration is any occurrence of the substructure in question in the graph; it is defined only by its edges, not by its edges and non-edges. See Fig. 2 for an example based on one from Fodor *et al.* [25, Fig. 5B].

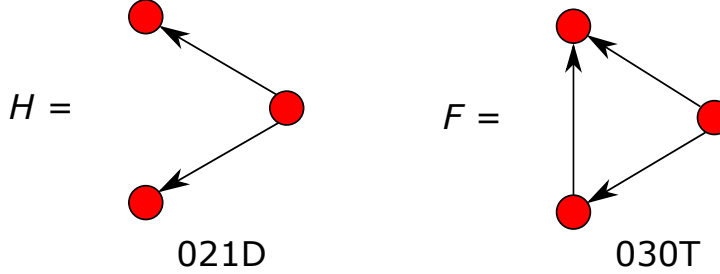


Figure 2: Motif examples. F , the transitive triangle (triad 030T) is not a special case of H , the out-star (triad 021D), when considered as motifs (or triad census classes): they are distinct induced subgraphs of three nodes. However, when considered as ERGM configurations, since H is a subgraph (but not an induced subgraph) of F (the transitive triangle is formed by “closing” the out-star with an additional arc), in their corresponding statistics both F and H are counted for an occurrence of F .

ERGMs solve the problem of the need to correct for correlations between motif occurrences, and also other attributes such as subcellular location (functional and evolutionary significance is another matter entirely). Given an observed network, model parameters can be estimated by maximum likelihood. Hence parameters corresponding to candidate motifs such as triangles can be estimated, and a positive significant parameter would indicate triangles occurring more frequently than by chance, *given the other parameters in the model* (which would include parameters to control for density and degree distribution, for example). ERGMs allow different structural configurations to be incorporated, as well as configurations based on node attributes (such as physico-chemical properties, or spatial locality), and the significance of the configurations can then be assessed given all the other structural and other configurations included in the model.

ERGMs fulfill all of the desirable criteria for improved network models listed by de Silva & Stumpf [52, p. 427]. They take into account that networks are finite. Indeed, far from requiring very large networks to fit the requirements of mean-field theories, they are dependent on network size and do not scale consistently to infinity [53–55] — a property that can be used to estimate population size from network samples [56]. They can handle modular organization or community or block structure [57–62], samples from larger networks [63–65], and missing data [66, 67]. And finally, they are flexible at incorporating additional information such as nodal attributes, including dyadic attributes, such as distances between nodes. ERGMs have also been extended to handle valued networks [68, 69] and dynamic (time-varying) networks [70], and to use graphlets [71] as the ERGM configurations [72].

Despite these potential advantages, however, ERGM parameter estimation is a computationally intractable problem, and in practice it is generally necessary to use Markov chain Monte Carlo (MCMC) methods [73]. A variety of algorithms for ERGM model fitting [74–77] are implemented in widely used software packages such as statnet [78–80] and PNet/MPNet [81], and Bayesian methods are also available [82, 83]. These packages also implement the so-called “alternating” or “geometrically weighted” configurations [84, 85], which alleviate problems with model “near-degeneracy”, where the model’s probability mass is concentrated in a very small region of possible networks, which can occur when only simple configurations, such as stars and triangles, are used [73].

Until recently, the computational difficulty of ERGM parameter estimation has limited its application to biological networks, which are often larger than the social networks (traditionally measured by observations and surveys, rather than online social networks) for which the techniques were developed. Now, however, advances such as snowball sampling and conditional estimation [64, 65], improved ERGM distribution samplers such as the “improved fixed density” (IFD) sampler [43], and new estimation algorithms [76], including the “Equilibrium Expectation” (EE) algorithm [44, 45] and its implementation for large directed networks [46], have reduced by orders of magnitude the time taken to estimate ERGM parameters.

3 Literature review of application of ERGMs to biological networks

ERGMs were first applied to biological networks by Saul & Filkov [14], who estimated model parameters for *Escherichia coli* [86] and yeast regulatory networks, and a collection of metabolic networks. With the algorithms and implementations available at the time, the larger networks could only be estimated by maximum pseudo-likelihood [87], an approximation which is now considered problematic [73, 85, 88] and useful mostly for obtaining initial parameter estimates for a more accurate (but also more computationally expensive) method [75–77]. Further, all the networks in Saul & Filkov [14] were treated as undirected, thereby losing important directional information (and not, for example, being able to distinguish between cyclic and transitive triads) in regulatory networks. The *E. coli* regulatory network, treated as undirected, was also used as an example application of the “stepping” algorithm for ERGM estimation by Hummel *et al.* [76].

Exponential random graph models for similar *E. coli* regulatory networks were described by Begum *et al.* [89], leaving the networks directed rather than treating them as undirected. These models were very simple, however, including only Arc and In-star terms.

Bayesian estimation of an ERGM model of a human PPI network with 401 proteins was described by Bulashevska *et al.* [90]. This model used only very basic structural features (not including any triangular structures, for example), but made use of nodal attributes, specifically a binary variable indicating if the protein is disordered. This ERGM was not used to analyze network motifs, but rather the relationship between disordered proteins and their “sociality”, a measure of their importance in the PPI network, finding that intrinsically disordered proteins tend to be more “social” [90]. In their Conclusions, Bulashevska *et al.* [90] suggest that “The ERGM modelling of networks offers a natural way of assessing importance of the network motifs” [90, p. 13].

Similar techniques, that is, Bayesian estimation of ERGMs with only very simple structural terms, have also been used with gene-gene relationship networks to model mechanisms of gene dysregulation [91].

A mixture ERGM was introduced by Wang *et al.* [60] and applied to a yeast gene interaction network with 424 genes [60, 92]. The advantage of the mixture ERGM is that it captures heterogeneity in clusters found in the network, but we do not address cluster or community structure here.

ERGMs have been applied to neural networks with 90 nodes, representing brain regions [93, 94], and more recently using Bayesian techniques, with 96 nodes representing such regions [95]. ERGMs have also been used to model human brain networks inferred from electroencephalographic (EEG) signals; these networks have 56 (the number of EEG sensors) nodes [96]. An enhanced version of the generalized (or valued) ERGM [68] was used to model the human Default Mode Network (DMN) with 20 nodes, representing brain regions [97]. This latter work is an example of an ERGM that incorporates spatial distances, in the form of three-dimensional Euclidean distances between nodes.

A Bayesian ERGM has been used to model transient structure in intrinsically disordered proteins [98], and a specific family of ERGMs has been used to model amyloid fibril topologies [99].

Simple ERGMs for undirected networks (*A. thaliana*, yeast, human, and *C. elegans* PPI networks, and undirected versions of *E. coli* regulatory and *Drosophila* optic medulla networks) were estimated in Byshkin *et al.* [44, S.I.], demonstrating that the EE algorithm could be used to estimate in minutes a model that takes many hours or is practically impossible with earlier methods. In addition, a more complex model of the *A. thaliana* PPI network was estimated, showing not just the over-representation of the triangle motif, but also the tendency for plant-specific proteins to interact preferentially with each other, and for kinases to interact preferentially with phosphorylated proteins [44]. However that work dealt only with undirected networks. An implementation of the EE algorithm for directed networks was described in Stivala *et al.* [46], but no biological networks were considered in that work.

4 Methods

4.1 Network data

We obtained a yeast PPI network [39] from the igraph [17] Nexus network repository (this is no longer available, we used the network downloaded on 10 November 2016). The yeast PPI network has the proteins annotated with one of 12 functional categories [100, 101] (or “uncharacterized”), as described in the Supplementary Information of von Mering *et al.* [39].

The previously mentioned *E. coli* regulatory network [4, 86] was obtained via the statnet package [78, 102]. Following Hummel *et al.* [76], we removed the loops (self-edges) representing self-regulation, and considered self-regulation instead in a simplistic way by a binary node attribute designated “self” which is true when a self-loop was present and false otherwise. We also obtained a *Saccharomyces cerevisiae* (yeast) regulatory network [3, 103] (<http://www.weizmann.ac.il/mcb/UriAlon/download/collection-complex-networks>; accessed 29 April 2019) and processed it in the same way.

For all networks we removed multiple edges and self-loops, where present.

Summary statistics of the networks are in Table 1 and the degree distribution of the undirected network is shown in Fig. 3, and for the directed networks, Fig. 4. Power law and log-normal distributions were fitted using the methods of Clauset *et al.* [104] implemented in the powerLaw package [105].

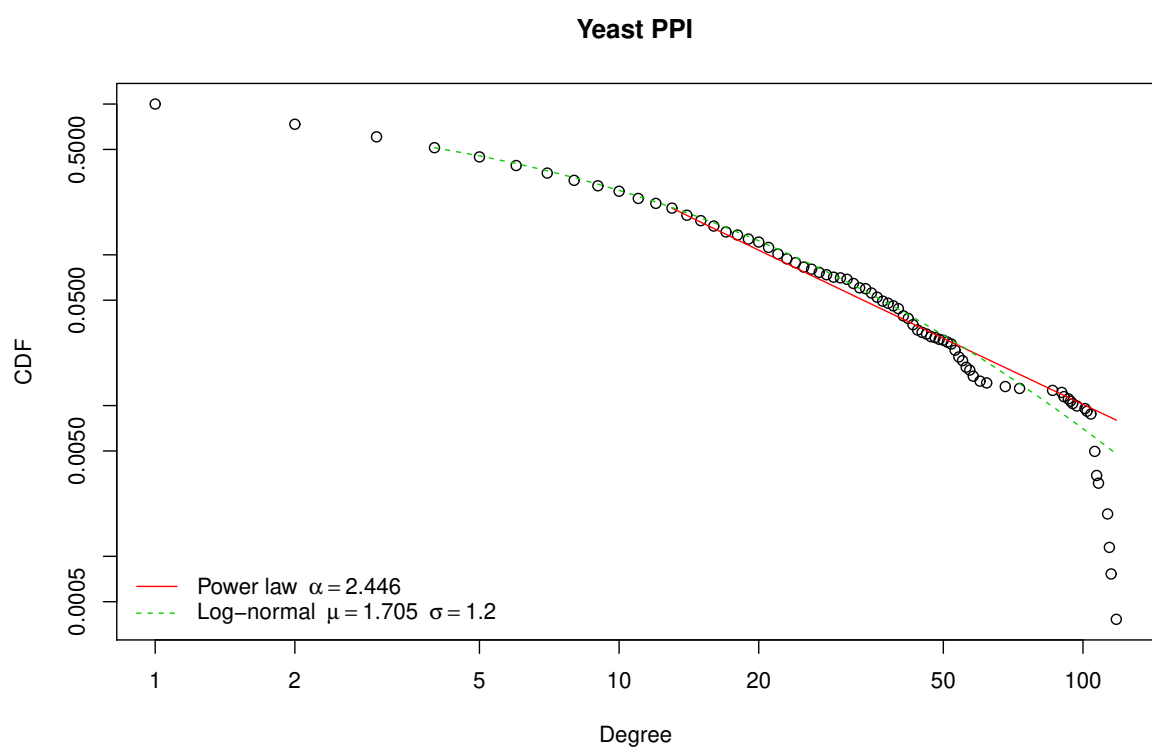


Figure 3: Degree distribution of the yeast PPI network. The degree distribution is consistent with a log-normal but not a power law distribution ($p < 0.001$).

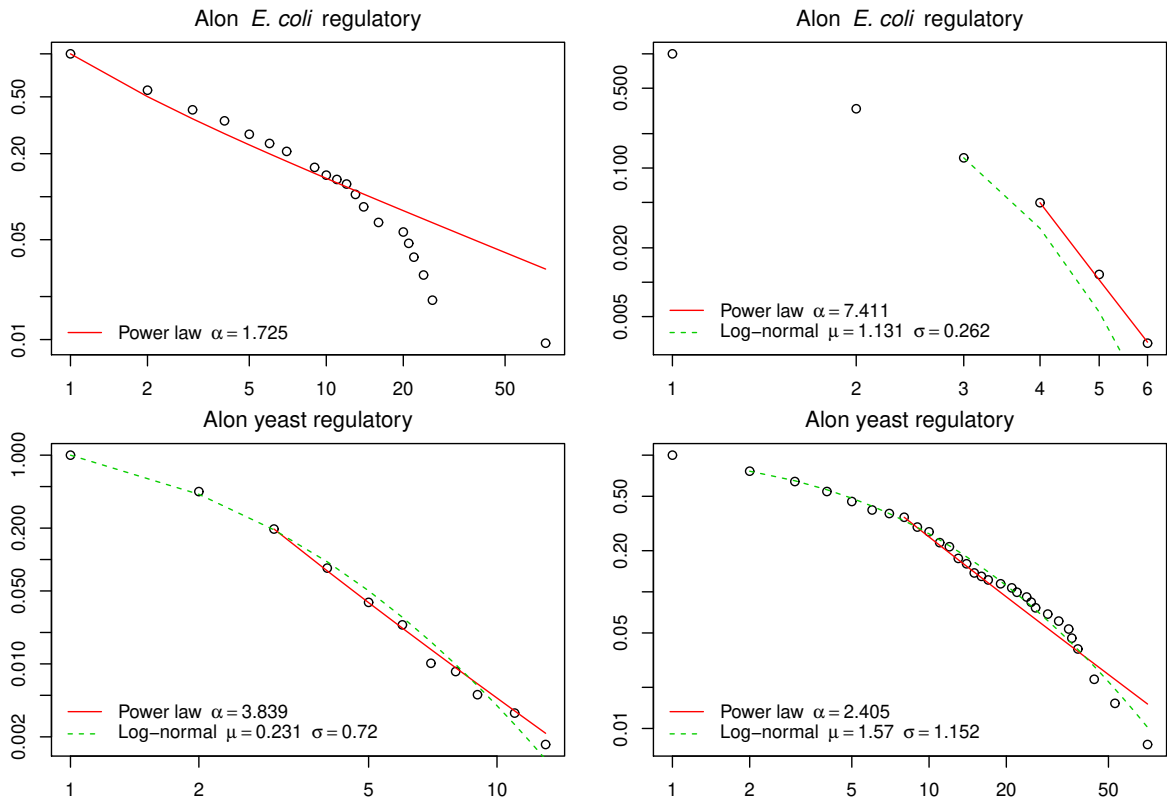


Figure 4: Degree distributions for directed networks. Power law and log-normal distributions fitted to the CDF for (left) in- and (right) out-degree distributions of the directed networks. All distributions apart from the *E. coli* in-degree distribution (for which a log-normal distribution could not be fitted) are consistent with both power law and log-normal distributions.

Table 1: Summary statistics for the biological networks. “Clustering coefficient” is the global clustering coefficient (transitivity).

Network	Directed	Nodes	Edges	Density	Clustering coefficient
Yeast PPI	No	2617	11855	0.00346	0.46862
Alon <i>E. coli</i> regulatory	Yes	423	519	0.00291	0.02382
Alon yeast regulatory	Yes	688	1079	0.00228	0.01625

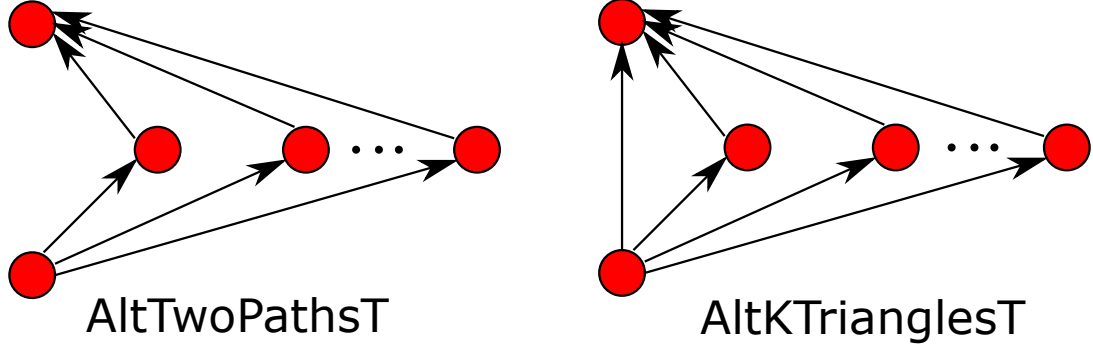


Figure 5: Alternating two-paths and alternating transitive triangles ERGM configurations for directed networks. Unlike motifs, ERGM configurations are not induced subgraphs, so it is normal (and often required) for one to be a subgraph of another. So AltTwoPathsT and AltKTrianglesT are frequently included in a model together, with AltKTrianglesT consisting of the AltTwoPathsT configuration “closed” by the addition of an arc.

Table 2: Parameters for undirected networks.

Effect	Description
Edge	Baseline density
A2P	Alternating k -two-paths. Used as a “control” for alternating k -triangles.
AS	Alternating k -stars. A positive parameter value indicates centralization based on high-degree nodes.
AT	Alternating k -triangles. A positive parameter value indicates network closure (triangles).
Match c	Categorical matching on categorical attribute c . A positive parameter value indicates an edge preferentially forming between nodes with the same value of the categorical attribute (known as “homophily” in social network research).

4.2 ERGM configurations

The ERGM parameters used in the models for undirected networks are shown in Table 2, and those for directed networks in Table 3. Detailed descriptions of these parameters and their corresponding statistics can be found in [46–48, 84, 85, 106], but two of the important ones used in this work are shown in Fig. 5.

The “alternating” statistics [48, 84, 85] such as alternating k -stars involve sums of counts of configurations with alternating signs and a decay factor λ , and, except where otherwise specified, we set $\lambda = 2$ in accordance with common ERGM modeling practice.

4.3 ERGM parameter estimation

ERGM parameters for undirected networks were estimated using the EE algorithm [44] with the IFD sampler [43] implemented for undirected networks in the Estimnet software as described in Byshkin *et al.* [44], with 20 estimations (run in parallel). ERGM parameters for directed networks were estimated using the simplified EE algorithm [44, 45] with IFD sampler implemented for directed networks in the EstimNetDirected software [46], with 64 estimations (run in parallel).

The Alon *E. coli* network does not contain any reciprocated arcs (directed loops of length two), and so estimation is made conditional on this by preventing the creation of reciprocated arcs in the MCMC procedure.

Table 3: Parameters for directed networks.

Effect	Description
Arc	Baseline density.
Sink	A positive parameter value indicates a tendency for nodes with incoming but no outgoing arcs.
Source	A positive parameter value indicates a tendency for nodes with outgoing but no incoming arcs.
Reciprocity	A positive parameter value indicates a tendency for arcs to be reciprocated (a cycle of length 2).
AltInStars	Alternating k -in-stars. A positive parameter value indicates centralization based on high in-degree nodes.
AltOutStars	Alternating k -out-stars. A positive parameter value indicates centralization based on high out-degree nodes.
AltTwoPathsT	Multiple 2-paths. A positive parameter value indicates a tendency for directed paths of length 2. Used as a “control” for AltKTrianglesT, the parameter for triangles formed by closing these 2-paths.
AltKTrianglesT	Path closure or transitive closure. A positive parameter value indicates a tendency for open directed two-paths to be closed transitively. This is an alternating statistic version of the “feed-forward loop” motif.
AltKTrianglesC	Cyclic closure. A positive parameter value indicates a tendency for directed cycles of length 3 in the network, representing non-hierarchical network closure. An alternating statistic version of the “three-node feedback loop” motif.
Sender a	Sender on binary attribute a . A positive parameter value indicates that nodes with the attribute are more likely to have an incident arc directed from them.
Receiver a	Receiver on binary attribute a . A positive parameter value indicates that nodes with the attribute are more likely to have an incident arc directed to them.
Interaction a	Interaction on binary attribute a . A positive parameter value indicates that two nodes which both have the attribute are more likely to have an arc directly connecting them.
Matching c	Matching on categorical attribute c . A positive parameter value indicates that two nodes which have the same value of the attribute are more likely to have an arc directly connecting them.

4.4 Convergence and goodness-of-fit tests

Convergence was tested as described in [44, 46], by requiring the absolute value of each parameter’s t-ratio to be no greater than 0.3, and by visual inspection of the parameter and statistic trace plots. For the directed networks estimated with EstimNetDirected, an additional heuristic convergence test was used, as described in [46]. Observed graph statistics were plotted on the same plots as the distributions of those statistics in the networks simulated in the EE algorithm MCMC process, to check that they do not diverge. The statistics used are the same as those of the actual goodness-of-fit test described below, but note that this test is only for estimation convergence, not goodness-of-fit [46].

For the directed networks estimated with EstimNetDirected, a simulation-based goodness of fit procedure was used, similar to that used in statnet [80]. A set of networks was simulated from the estimated model (using the SimulateERGM program in the EstimNetDirected software), and the distribution of certain graph statistics compared with those of the observed network by plotting the observed network values on the same plots as the distribution of simulated values. The statistics used were the in- and out-degree distributions, reciprocity, giant component size, mean local and global clustering coefficients, triad census, geodesic distance (shortest path length) distribution, and edgewise and dyadwise shared partners distributions.

Source code, configuration files, and datasets are available from https://sites.google.com/site/alexdstivala/home/ergm_bionetworks.

5 Results and discussion

Table 4 shows the basic structural model for the yeast PPI network (Model 1), a model with the alternating k -two-paths (A2P) parameter added (Model 2), as well as a model (Model 3) incorporating a parameter for the propensity of interactions to occur between proteins in the same functional category (class). Model 1 reproduces a model of this network in a previous work [44,

Table 4: Parameter estimates with 95% confidence interval for the yeast PPI network, from the EE algorithm. Parameter estimates that are statistically significant are shown in bold.

Effect	Model 1	Model 2	Model 3
Edge	-7.758 (-7.806, -7.709)	-10.667 (-10.685, -10.650)	-9.282 (-9.302, -9.262)
AS	-0.048 (-0.103, 0.007)	1.077 (1.013, 1.140)	0.604 (0.550, 0.659)
A2P	—	-0.087 (-0.090, -0.084)	-0.059 (-0.062, -0.056)
AT	1.857 (1.807, 1.907)	2.511 (2.474, 2.548)	2.432 (2.396, 2.467)
Match class	—	—	0.358 (0.315, 0.402)

Table 5: Parameter estimates with 95% confidence interval for the Alon *E. coli* regulatory network. Parameter estimates that are statistically significant are shown in bold.

Effect	Model 1	Model 2	Model 3
Arc	-8.208 (-8.368, -8.047)	-8.039 (-8.210, -7.869)	-7.670 (-7.830, -7.509)
Sink	3.295 (-0.240, 6.830)	2.991 (-0.140, 6.122)	2.877 (0.306, 5.448)
Source	1.238 (-1.770, 4.247)	1.472 (-1.787, 4.731)	1.546 (-1.063, 4.156)
AltInStars	2.587 (0.943, 4.232)	2.332 (0.539, 4.126)	2.299 (0.555, 4.044)
AltOutStars	-1.001 (-2.363, 0.362)	-0.901 (-2.454, 0.652)	-0.848 (-1.885, 0.189)
AltTwoPathsT	-0.170 (-0.638, 0.297)	-0.144 (-0.612, 0.323)	-0.165 (-0.603, 0.272)
AltKTrianglesT	2.885 (0.798, 4.972)	2.814 (0.758, 4.869)	2.830 (1.025, 4.636)
Sender self	—	-0.463 (-4.140, 3.214)	—
Receiver self	—	0.346 (-0.506, 1.199)	—
Interaction self	—	-0.119 (-3.722, 3.484)	—
Matching self	—	—	-0.451 (-1.181, 0.280)

Table S3]; Models 2 and 3 are new.

Each of these model estimations took approximately 7 minutes total elapsed time on cluster nodes with Intel Xeon E5-2650 v3 2.30GHz processors using 20 parallel tasks.

We expect that proteins of the same functional category should preferentially interact with each other [39], and this is confirmed by the significant positive parameter estimated for the “Match class” effect. The alternating k -triangle (AT) parameter is positive and significant in all models, showing an over-representation of triangles (which we might expect given the very high value of the clustering coefficient for this network, Table 1), even in models also including parameters for two-paths and preferential interaction of proteins in the same class.

We estimated three different models of the Alon *E. coli* regulatory network (Table 5). As in Hummel *et al.* [76], we modeled self-regulation by using a nodal covariate “self” which is true exactly when the node had a self-loop in the original network. These ERGM models are new, in that previous work with ERGMs on these networks either treated them as undirected [14, 76], thereby ignoring the inherently directed nature of such a regulatory network; or, in the case where the network was left as directed, included only Arc and alternating k -in-stars terms, as the estimation methods used at the time could not find converged models when other terms, such as triangles, were included [89].

Each of these model estimations took approximately three minutes total elapsed time on cluster nodes with Intel Xeon E5-2650 v3 2.30GHz processors using 64 parallel tasks.

In these models, the Sink and Source parameters are used to control, respectively, for the presence of genes that do not regulate any genes (have out-degree zero) and genes that are not regulated by any gene (have in-degree zero). The alternating k -in-stars (AltInStars) parameter is consistently positive and significant, indicating significant skewness of the in-degree distribution, that is, the presence of “hubs” with higher in-degree than other nodes. There is no significant effect for (or against) such skewness of the out-degree distribution (see Fig. 4 and Fig. 6).

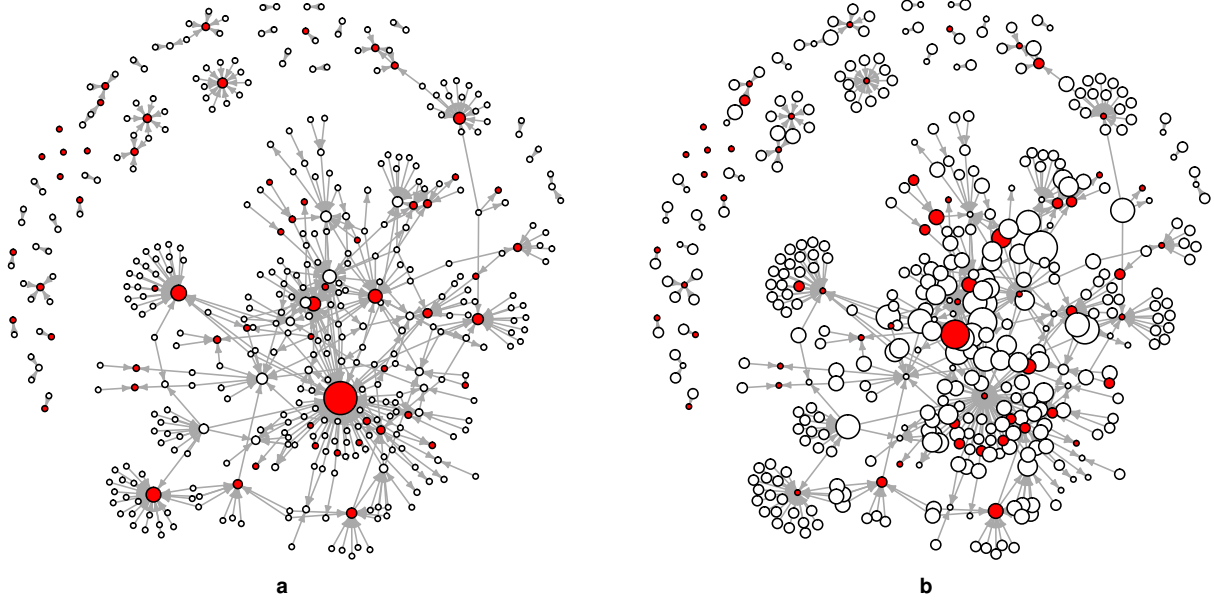


Figure 6: Alon *E. coli* regulatory network. (a) Node size is proportional to in-degree. (b) Node size is proportional to out-degree. Self-regulating operons are depicted as filled (red) circles. In (a) there appears to be a small set of high in-degree nodes and a much larger set of smaller in-degree nodes, while in (b) the out-degree of the nodes appears to be much more evenly distributed. The hypothesis we might make from (a), that there is centralization on in-degree, is confirmed by the ERGM results. This same model finds no support for the hypothesis we might make from (b), that there is a tendency against centralization on out-degree.

The only other parameter that is consistently significant (and positive) is path closure (AltKTrianglesT), which we can interpret as a significant tendency for the “feed-forward loop” to be over-represented, consistent with the results in Milo *et al.* [3].

A goodness-of-fit plot for this model is shown in Fig. B.9, showing a good fit for the model (Model 1 is used as Models 2 and 3 have no additional statistically significant parameter estimates). A goodness-of-fit plot for the triad census (Fig. 7) shows that the model reproduces the triad census well, and specifically triad 030T, the transitive triad (three node feed-forward loop), giving additional confidence that the positive and statistically significant AltKTrianglesT parameter is evidence for over-representation of this motif, given the other parameters in the model.

Note that this *E. coli* regulatory network does not contain any instances of the three-cycle, or “three-node feedback loop” [3]. Indeed the Alon *E. coli* network does not contain any loops greater than size one [4], and so the cyclic closure parameter (AltKTrianglesC) is not included in the models.

Table 6 shows ERGM parameter estimates for the Alon yeast regulatory network. Each of these model estimations took approximately three minutes total elapsed time on cluster nodes with Intel Xeon E5-2650 v3 2.30GHz processors using 64 parallel tasks. These ERGM models are also new; previously published ERGMs for similar networks having treated them as undirected [14].

In Model 1 (Table 6), estimation is conditional on no reciprocated arcs, just as was done for the *E. coli* regulatory network. However in this yeast regulatory network, there is actually a single reciprocated arc (two-cycle) in the data, and hence the fit of the model on statistics involving reciprocated arcs is poor. This is apparent, for example, in the poor fit for triad census class 102 (triad with only a mutual arc) in Fig 8, or for the reciprocity statistic in the goodness-of-fit plot (Fig B.10). The fit for other statistics, and in particular the degree and shared partner distributions, is acceptable (with the exception of poor fit on the giant component size). Importantly, the fit on the triad census class 030T (transitive triad) is good (Fig. 8).

In order to better model reciprocity, a model (Model 2 in Table 6) was estimated without being conditional on there being no reciprocated arcs, but without a reciprocity term in the model. This model also has adequate goodness-of-fit, but this time including good fit on the reciprocity statistic (Fig. B.11). It does, however, for some triads involving reciprocated arcs (120U for example), generate significantly more such triads than are observed in the data (Fig B.12). Therefore, a third model (Model 3 in Table 6) was estimated, including the Reciprocity parameter. However, probably due to the fact that the data contains only a single reciprocated arc, this model has a very large estimated standard error for the Reciprocity parameter. Further, it exhibits poor convergence with respect to the Reciprocity statistic, with a t-ratio greater than the maximum value of 0.3 we consider acceptable, since the data contains exactly one reciprocated arc, yet the model most frequently generates networks with none.

Model 1 and Model 2, therefore, are preferable. Nevertheless, in all three models, the sign and significance of estimated parameters (except Reciprocity) are the same. There is a positive and significant parameter for alternating k -out-stars (AltOut-

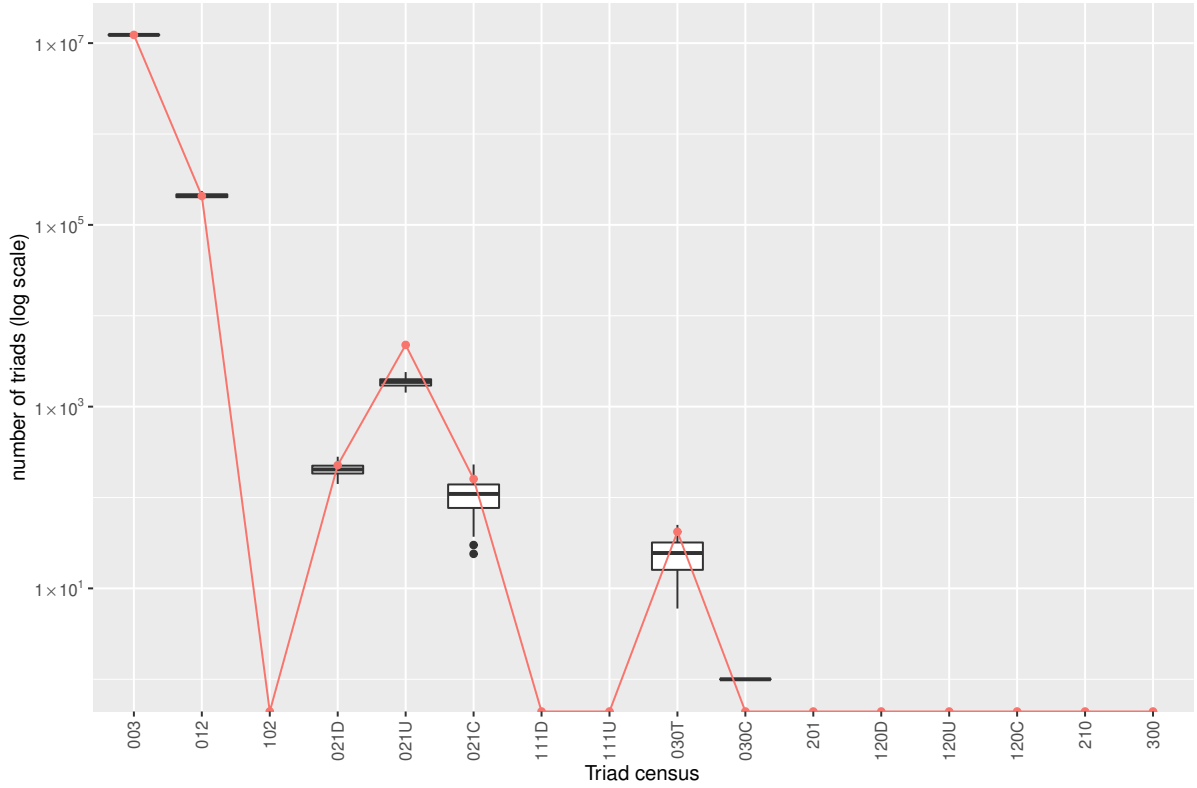


Figure 7: Goodness-of-fit plots for the triad census of the Alon *E. coli* regulatory network, Model 1 (Table 5). The observed triad counts are plotted in red with the triad counts of 100 simulated networks plotted as black boxplots. Because the triad counts (y -axis) are on a log scale, values of zero are omitted (observed zero counts shown as a red point on the bottom of the graph). For triad census class 030C (cyclic triad), the “box plot” consisting of a single median line for the simulated count represents a single (out of 100 simulations) occurrence of a nonzero count (of 1) for 030C.

Table 6: Parameter estimates with 95% confidence intervals for the Alon yeast regulatory network. Parameter estimates that are statistically significant are shown in bold. In Model 1 only, estimation is conditional on no reciprocated arcs, even though there is a single reciprocated arc in the data. Model 3 is included for illustration, even though it shows poor convergence with respect to the Reciprocity parameter (t-ratio magnitude is greater than 0.3).

Effect	Model 1	Model 2	Model 3
Arc	-7.489 (-7.665, -7.313)	-7.490 (-7.662, -7.318)	-7.490 (-7.667, -7.313)
Reciprocity	—	—	-6.114 (-15.535, 3.307)
AltInStars	-0.463 (-1.504, 0.577)	-0.435 (-1.451, 0.581)	-0.452 (-1.472, 0.568)
AltOutStars ($\lambda = 4.5$)	1.008 (0.756, 1.261)	1.006 (0.757, 1.256)	1.008 (0.752, 1.264)
AltTwoPathsT ($\lambda = 3$)	-0.332 (-0.739, 0.076)	-0.298 (-0.670, 0.074)	-0.315 (-0.684, 0.054)
AltKTrianglesT ($\lambda = 3$)	2.297 (0.484, 4.111)	1.842 (0.043, 3.640)	2.121 (0.479, 3.763)

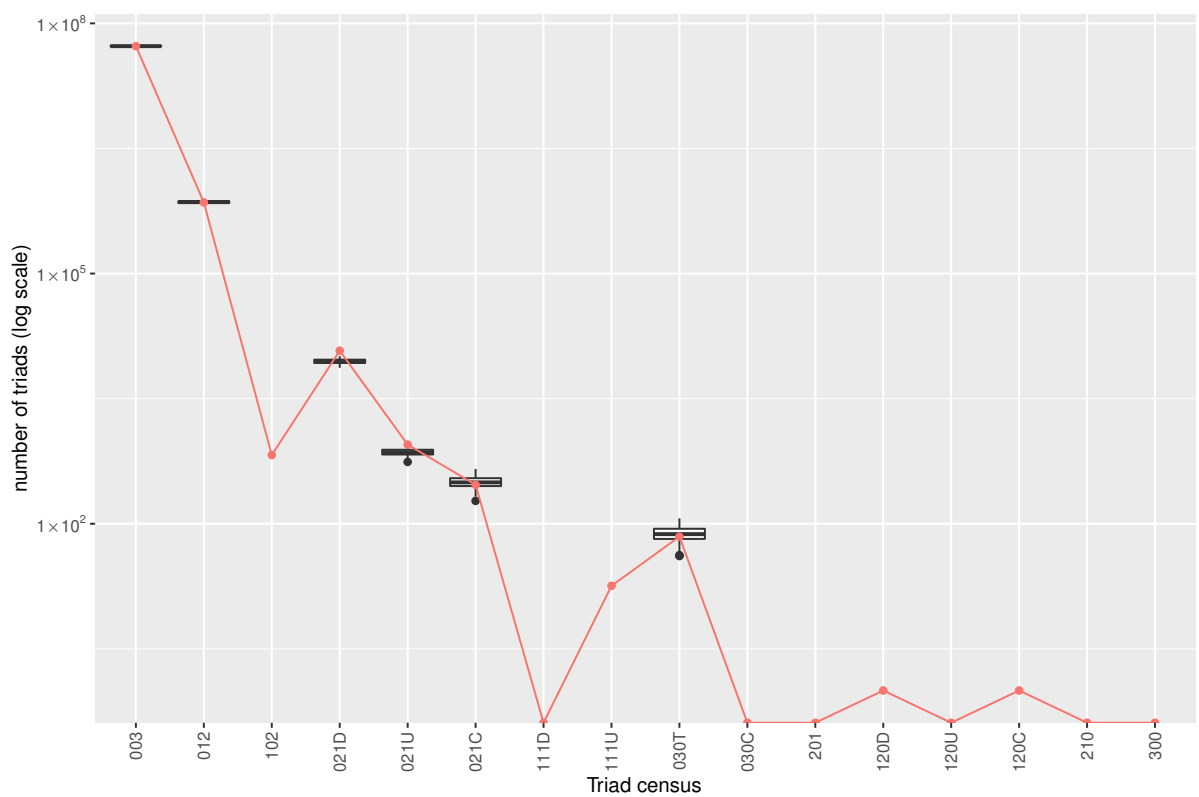


Figure 8: Goodness-of-fit plots for the triad census of the Alon yeast regulatory network, Model 1 (Table 6). The observed triad counts are plotted in red with the triad counts of 100 simulated networks plotted as black boxplots.

Stars), indicating the presence of “hubs” with higher out-degree than other nodes. This is as we might expect from Fig. 4, and contrasts with the *E. coli* regulatory network, which has in-degree hubs but not out-degree hubs.

Also in all three models, there is a positive and significant parameter estimate for transitive closure (AltKTrianglesT). Given this estimate, and the good fit for the transitive closure motif 030T (Fig 8) we can again interpret this as a significant over-representation of this motif (“feed-forward loop”), consistent with the results of Milo *et al.* [3].

In all three models in Table 6, the decay parameter λ for the “alternating” statistics has been set to a value other than the default $\lambda = 2$ for alternating k -out-stars (AltOutStars), multiple two-paths (AltTwoPathsT), and transitive closure (AltKTrianglesT). This is because models initially estimated with the default $\lambda = 2$ value (Table A.7) showed poor goodness-of-fit on the out-degree distribution (Fig B.13) and triad census class 030T (Fig B.14). Therefore, new models were estimated with a higher value of λ for the alternating k -out-star parameter to assist with modeling the highly skewed out-degree distribution [107], and also a higher value of λ for AltTwoPathsT and AltKTrianglesT (the same value of λ for both) to aid model convergence and fit for transitivity [84].

The cyclic triangle structure has been suggested as an “anti-motif” (i.e. occurs less frequently than expected), but in some cases its apparent under-representation has been shown to be an expected consequence of other topological properties of biological networks [23]. In the examples used here, there were so few (or no) occurrences of this motif, that models including the corresponding parameter (in the form of the AltKTrianglesC parameter) would not converge. Yet the networks simulated from these models also contain no (or very few) occurrences of this candidate anti-motif. This is consistent with the lack of cyclic triangles not being due to cyclic triangles being an anti-motif as such, but rather as a consequence of the other topological features of the network, and specifically in these examples, the features described by the parameters included in the models.

6 Limitations

Finding a converged ERGM for a network is not always possible in practice. In particular, models which include Markov dependency assumption parameters such as triangles, corresponding directly to three-node motif candidates such as three-node feed-forward-loops (transitive triangles) and three-cycles, for example, usually do not converge. For this reason it is normal practice in ERGM modeling to use geometrically weighted or “alternating” configurations to solve this problem [73, 84, 85], as we did in this work. However this means we are not answering precisely the same question as when we ask directly if a motif is over-represented or not. This is because ERGM is a model for tie (edge or arc) formation, not for motif formation: if we consider ERGM as a type of logistic regression, the outcome variable is the presence or absence of a network tie. The predictor variables are not independent of each other, but form a nested hierarchy of configurations: triangles are formed by “closing” a two-path with an additional edge, for example. So a positive estimate of the alternating k -triangle parameter does not directly mean that the transitive triangle (three node feed-forward loop) motif is over-represented, but rather that there is tendency (that is, it is more probable than chance given the other parameters in the model) for three nodes forming a directed two-path to be closed in a transitive triangle. This makes sense in the social network origins of the model: it might be assumed to be the result in the observed network of the tendency of a person’s friends to also be friends with each other, for example. In the context of biological networks, it might be interpreted as a sign of evolutionary events, however this interpretation is very much open to question, as briefly discussed in the Introduction.

Hence in order to directly test motif significance, without having to fit a parameterized model such as ERGM, new methods, such as the “anchored motif” proposed by Fodor *et al.* [25] are still required

In some of the models presented here, we used values other than the usual default value $\lambda = 2$ for the decay parameter λ of the “alternating” statistics. We had to manually estimate appropriate values of λ based on trial and error, guided by knowledge of the observed network, convergence and goodness-of-fit of the models (or lack thereof), and the definitions of the relevant statistics [84, 107]. It is possible to instead estimate λ (or an equivalent parameter) directly from the data, as part of the model, using a “curved ERGM” [75, 108], and this is implemented in the statnet R package [78–80]. However it is not currently possible to estimate curved ERGMs using the EstimNetDirected software [46], and this is an area requiring further work.

As previously mentioned, the configurations available in an ERGM are determined by the dependence assumptions: although there is a lot of flexibility available in ERGM configurations, we cannot simply add arbitrary configurations without regard for the underlying dependency assumption [50]. The least restrictive assumption used in practice is the “social circuit” dependency assumption [48, 84, 85, 106] used in this work, which allows the use of the “alternating” configurations.

We also note that some recent work suggests that complex network structure, including heavy-tailed degree distributions, closure (clustering), large connected components, and short path lengths can arise simply from thresholding normally distributed data to generate the binary network [109]. Hence inferences from ERGM modeling about network structure, just as with other techniques such as comparison to ensembles of random graphs, could be consequences of the way the binary network was constructed.

Valued ERGMs [68, 69] may be used to avoid this problem by removing the need to construct a binary network at all, and working directly with the network with valued edges. Parameter estimation for these models is even more computationally intensive than for binary networks, and hence is so far impractical to use for networks of the size considered here. Using new estimation techniques to improve the scalability of parameter estimation for valued ERGMs is another area requiring further research.

For the relatively small (on the order of one thousand nodes or fewer) directed networks considered here, it is possible to do simulation-based goodness-of-fit tests. However, it is possible to estimate ERGM parameters for far larger (over one million node) networks using the EstimNetDirected software, but it is not practical to simulate such large networks from the model, and this is an area requiring further work [46].

7 Conclusion

We have re-examined the use of exponential random graph models for analyzing biological networks, an application first introduced in the bioinformatics literature by Saul & Filkov [14]. Advances in ERGM estimation methods since then have allowed more sophisticated models to be estimated for more and larger networks than was possible at the time, and they are now a more practical technique for making inferences about structural hypotheses in biological networks, potentially solving some of the problems inherent in conventional methods for testing motif over-representation. By using an ERGM, all configurations in the model are tested simultaneously, each conditional on all the others, rather than having to test one at a time with the other configurations fixed in a (more or less sophisticated, the choice of which is critical to the results) null model.

The ERGM models of the *Alon E. coli* network presented here are the first to retain the directed nature of the network and also include terms for triangular structures. They confirm the result of Milo *et al.* [3] that path closure (feed-forward loop) is over-represented, even when we include other, related, parameters in the model.

We also presented the first ERGM models of a yeast regulatory network retaining its inherently directed nature (rather than treating it as undirected). We find statistically significant over-representation of the transitive closure motif, just as Milo *et al.* [3] did in the same yeast regulatory network, using a simple randomization test.

The lack of the cyclic triangle (feedback loop) structure in the data, however, is reproduced by models that do not contain any parameter corresponding to this structure. This suggests that this structure is not an “anti-motif”, but rather that its lack is a consequence of the structural features of the networks, specifically degree distributions, two-paths, and transitive closure, that are included in the models.

Funding

This work was supported by Swiss National Science Foundation National Research Programme 75 [grant number 167326]; and Melbourne Bioinformatics at the University of Melbourne [grant number VR0261].

Table A.7: Parameter estimates with 95% confidence intervals for the Alon yeast regulatory network, with the default value $\lambda = 2$ for the “alternating” parameters. Parameter estimates that are statistically significant are shown in bold. Model 3 is included for illustration, even though it shows poor convergence with respect to the Reciprocity parameter (t-ratio magnitude is greater than 0.3).

Effect	Model 1	Model 2	Model 3
Arc	-10.578 (-10.820, -10.335)	-10.080 (-10.331, -9.828)	-10.093 (-10.342, -9.844)
Sink	3.124 (-3.407, 9.655)	3.039 (-3.644, 9.721)	3.003 (-3.637, 9.642)
Source	2.903 (-4.488, 10.295)	1.601 (-6.715, 9.917)	1.949 (-6.490, 10.389)
Reciprocity	—	—	-10.800 (-26.307, 4.707)
AltInStars	0.347 (-2.723, 3.416)	0.427 (-2.804, 3.658)	0.336 (-2.818, 3.490)
AltOutStars	2.860 (-0.278, 5.998)	2.585 (-0.515, 5.685)	2.637 (-0.537, 5.811)
AltTwoPathsT	—	-0.110 (-0.581, 0.360)	-0.149 (-0.607, 0.310)
AltKTrianglesT	1.227 (0.315, 2.139)	1.706 (-0.773, 4.185)	2.390 (0.011, 4.770)

A Supplementary tables

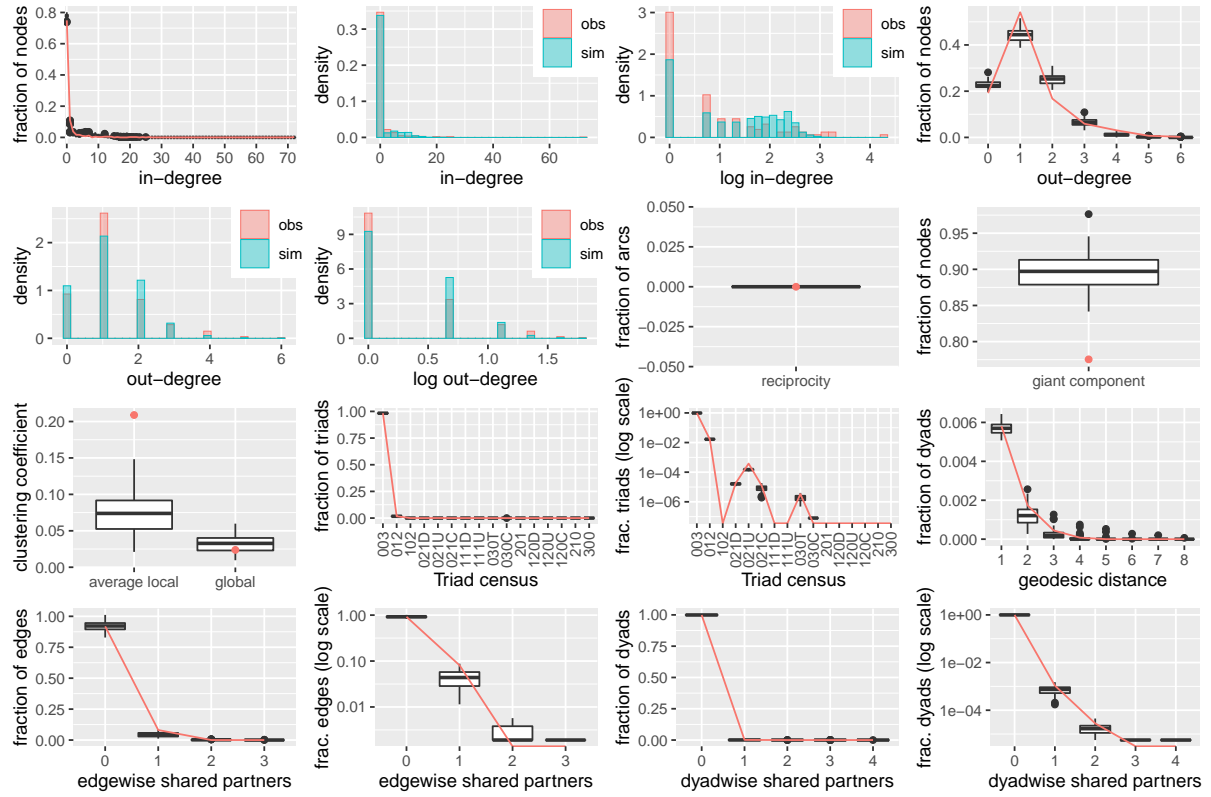


Figure B.9: Goodness-of-fit plots for the Alon *E. coli* regulatory network Model 1 (Table 5). The observed network statistics are plotted in red with the statistics of 100 simulated networks plotted as black boxplots, and blue on the histograms.

B Supplementary figures

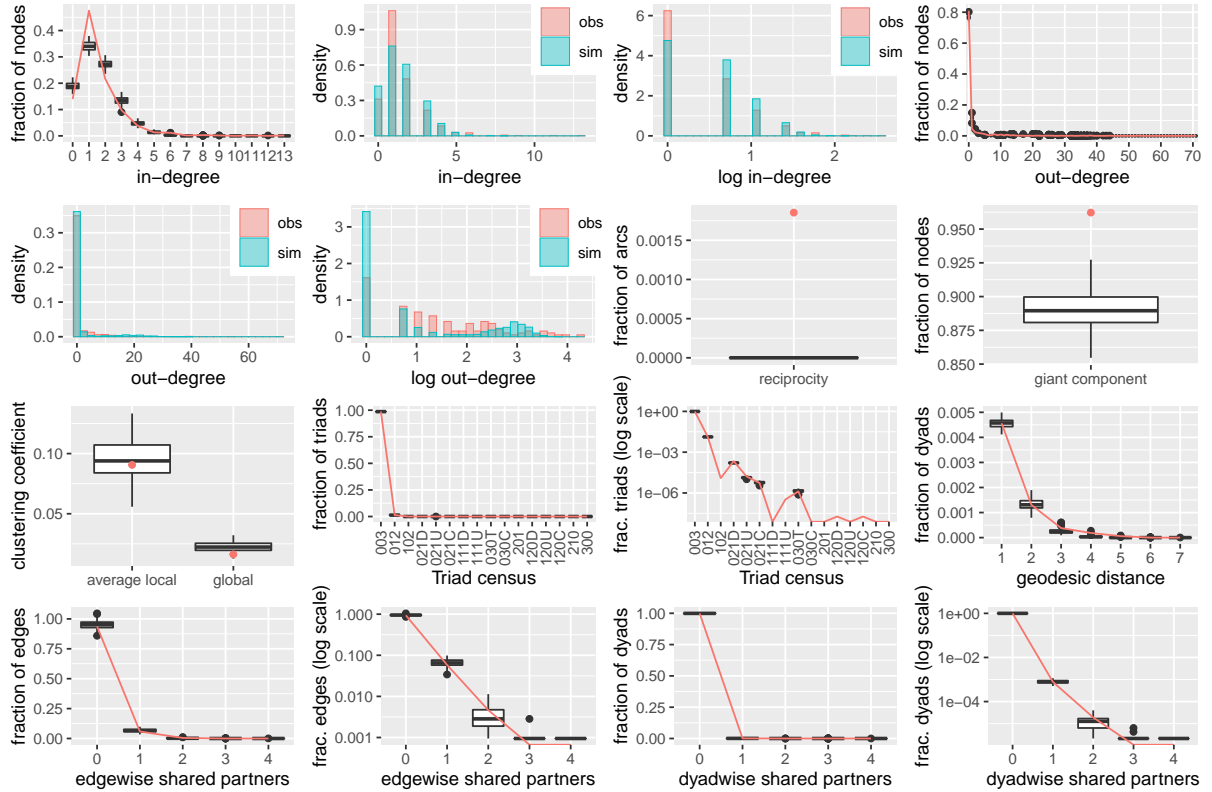


Figure B.10: Goodness-of-fit plots for the Alon yeast regulatory network Model 1 (Table 6). The observed network statistics are plotted in red with the statistics of 100 simulated networks plotted as black boxplots, and blue on the histograms.

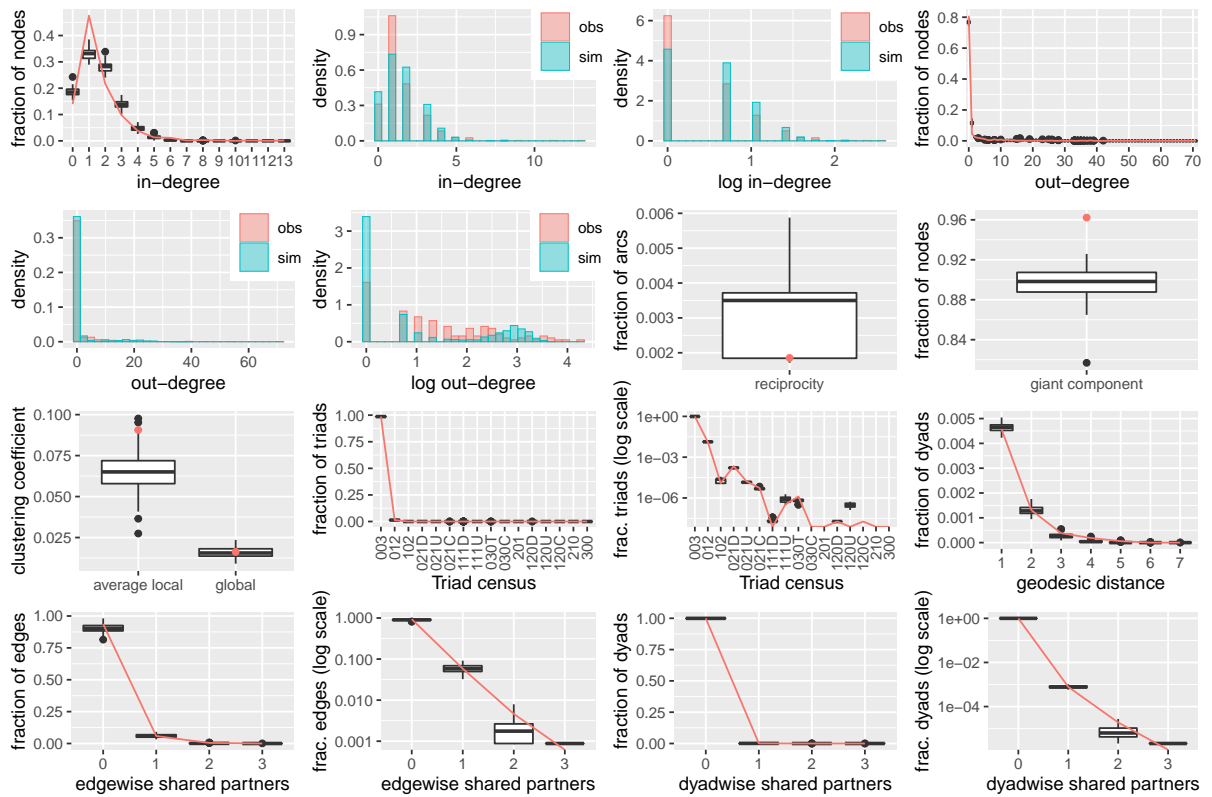


Figure B.11: Goodness-of-fit plots for the Alon yeast regulatory network Model 2 (Table 6). The observed network statistics are plotted in red with the statistics of 100 simulated networks plotted as black boxplots, and blue on the histograms.

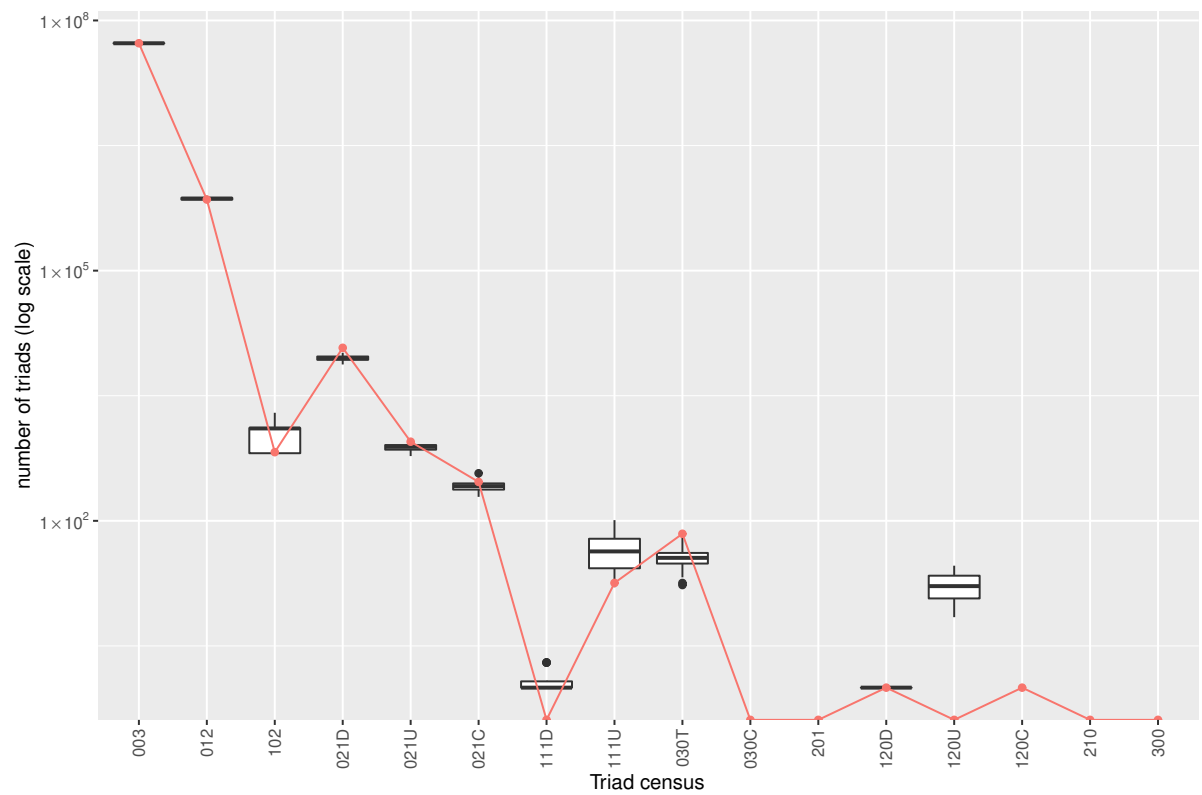


Figure B.12: Goodness-of-fit plots for the triad census of the Alon yeast regulatory network, Model 2 (Table 6). The observed triad counts are plotted in red with the triad counts of 100 simulated networks plotted as black boxplots.

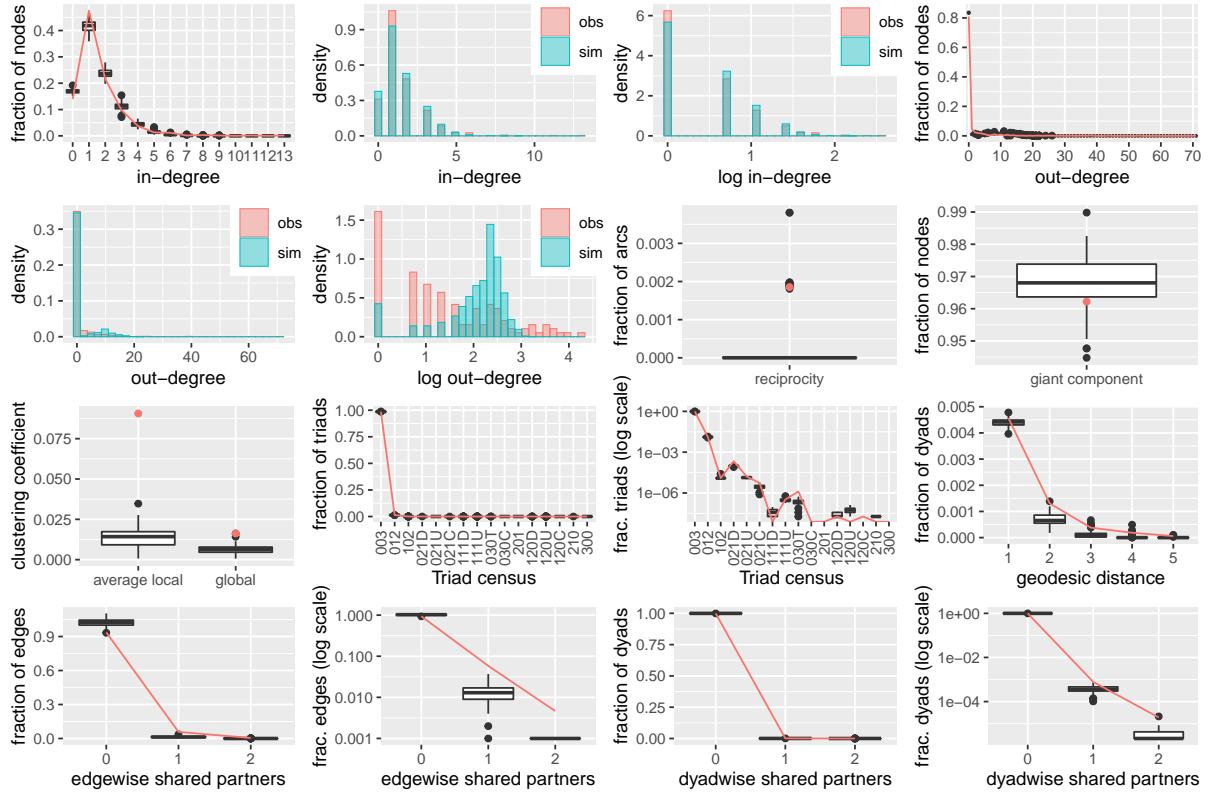


Figure B.13: Goodness-of-fit plots for the Alon yeast regulatory network Model 2 (Table A.7). The observed network statistics are plotted in red with the statistics of 100 simulated networks plotted as black boxplots, and blue on the histograms.

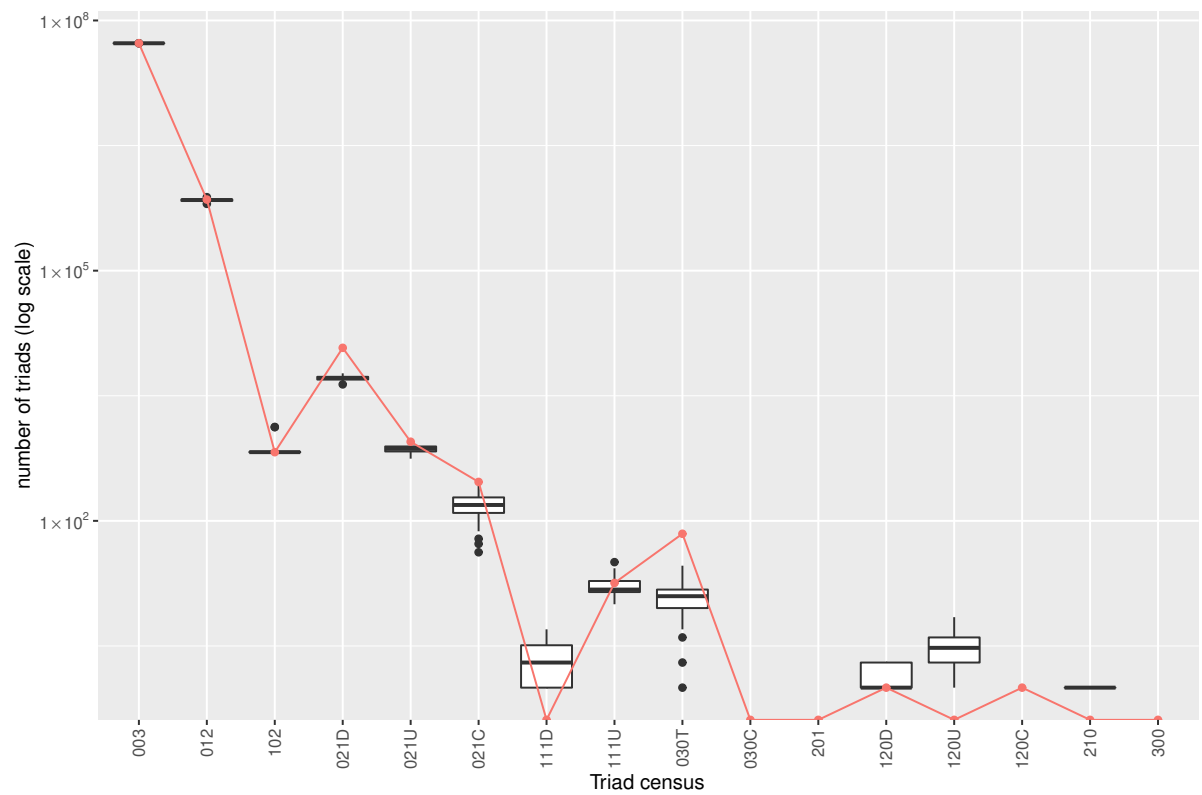


Figure B.14: Goodness-of-fit plots for the triad census of the Alon yeast regulatory network, Model 2 (Table A.7). The observed triad counts are plotted in red with the triad counts of 100 simulated networks plotted as black boxplots.

References

- [1] Winterbach, W., Van Mieghem, P., Reinders, M., Wang, H. & de Ridder, D. (2013) Topology of molecular interaction networks. *BMC Syst Biol*, **7**, 90.
- [2] De Las Rivas, J. & Fontanillo, C. (2010) Protein–protein interactions essentials: key concepts to building and analyzing interactome networks. *PLOS Comput Biol*, **6**(6), e1000807.
- [3] Milo, R., Shen-Orr, S., Itzkovitz, S., Kashtan, N., Chklovskii, D. & Alon, U. (2002) Network motifs: simple building blocks of complex networks. *Science*, **298**(5594), 824–827.
- [4] Shen-Orr, S. S., Milo, R., Mangan, S. & Alon, U. (2002) Network motifs in the transcriptional regulation network of *Escherichia coli*. *Nat Genet*, **31**(1), 64–68.
- [5] Alon, U. (2007) Network motifs: theory and experimental approaches. *Nat Rev Genet*, **8**, 450–461.
- [6] Ciriello, G. & Guerra, C. (2008) A review on models and algorithms for motif discovery in protein–protein interaction networks. *Brief Funct Genomics*, **7**(2), 147–156.
- [7] Middendorf, M., Ziv, E. & Wiggins, C. H. (2005) Inferring network mechanisms: the *Drosophila melanogaster* protein interaction network. *Proc Natl Acad Sci USA*, **102**(9), 3192–3197.
- [8] Rice, J. J., Kershenbaum, A. & Stolovitzky, G. (2005) Lasting impressions: motifs in protein–protein maps may provide footprints of evolutionary events. *Proc Natl Acad Sci USA*, **102**(9), 3173–3174.
- [9] Konagurthu, A. S. & Lesk, A. M. (2008) Single and multiple input modules in regulatory networks. *Proteins*, **73**(2), 320–324.
- [10] Davis, J. A. & Leinhardt, S. (1967) The structure of positive interpersonal relations in small groups.. In Berger, J., editor, *Sociological Theories in Progress*, volume 2, pages 281–251. Houghton Mifflin, Boston, MA.
- [11] Holland, P. W. & Leinhardt, S. (1970) A Method for Detecting Structure in Sociometric Data. *Am J Sociol*, **76**(3), 492–513.
- [12] Holland, P. W. & Leinhardt, S. (1976) Local structure in social networks. *Sociol Methodol*, **7**, 1–45.
- [13] Wasserman, S. & Faust, K. (1994) *Social network analysis: methods and applications*. Cambridge University Press, Cambridge.
- [14] Saul, Z. M. & Filkov, V. (2007) Exploring biological network structure using exponential random graph models. *Bioinformatics*, **23**(19), 2604–2611.
- [15] Moody, J. (1998) Matrix methods for calculating the triad census. *Soc Networks*, **20**(4), 291–299.
- [16] Batagelj, V. & Mrvar, A. (2001) A subquadratic triad census algorithm for large sparse networks with small maximum degree. *Soc Networks*, **23**(3), 237–243.
- [17] Csárdi, G. & Nepusz, T. (2006) The igraph software package for complex network research. *InterJournal, Complex Systems*, 1695.
- [18] Hagberg, A., Swart, P. & S Chult, D. (2008) Exploring network structure, dynamics, and function using NetworkX. In Varoquaux, G., Vaught, T. & Millman, J., editors, *Proceedings of the 7th Python in Science Conference (SciPy 2008)*, pages 11–16.
- [19] Lienert, J., Koehly, L., Reed-Tsochas, F. & Marcum, C. S. (2019) An efficient counting method for the colored triad census. *Soc Networks*, **58**, 136–142.
- [20] Faust, K. (2010) A puzzle concerning triads in social networks: Graph constraints and the triad census. *Soc Networks*, **32**(3), 221–233.
- [21] Picard, F., Daudin, J.-J., Koskas, M., Schbath, S. & Robin, S. (2008) Assessing the exceptionality of network motifs. *J Comput Biol*, **15**(1), 1–20.
- [22] Martorana, E., Micale, G., Ferro, A. & Pulvirenti, A. (2020) Establish the expected number of induced motifs on unlabeled graphs through analytical models. *Appl Netw Sci*, **5**(1), 58.
- [23] Konagurthu, A. S. & Lesk, A. M. (2008) On the origin of distribution patterns of motifs in biological networks. *BMC Syst Biol*, **2**, 73.

[24] Ginoza, R. & Mugler, A. (2010) Network motifs come in sets: Correlations in the randomization process. *Phys Rev E*, **82**(1), 011921.

[25] Fodor, J., Brand, M., Stones, R. J. & Buckle, A. M. (2020) Intrinsic limitations in mainstream methods of identifying network motifs in biology. *BMC Bioinformatics*, **21**, 165.

[26] Mayhew, B. H. (1984) Baseline models of sociological phenomena. *J Math Sociol*, **9**(4), 259–281.

[27] Anderson, B. S., Butts, C. & Carley, K. (1999) The interaction of size and density with graph-level indices. *Soc Networks*, **21**(3), 239–267.

[28] Butts, C. T. (2008) Social network analysis: A methodological introduction. *Asian J Soc Psychol*, **11**(1), 13–41.

[29] Snijders, T. A. B. (1991) Enumeration and simulation methods for 0–1 matrices with given marginals. *Psychometrika*, **56**(3), 397–417.

[30] Mahadevan, P., Krioukov, D., Fall, K. & Vahdat, A. (2006) Systematic topology analysis and generation using degree correlations. *ACM SIGCOMM Comp Com*, **36**(4), 135–146.

[31] Orsini, C., Dankulov, M. M., Colomer-de Simón, P., Jamakovic, A., Mahadevan, P., Vahdat, A., Bassler, K. E., Toroczkai, Z., Boguná, M., Caldarelli, G. et al. (2015) Quantifying randomness in real networks. *Nat Commun*, **6**, 8627.

[32] Mazurie, A., Bottani, S. & Vergassola, M. (2005) An evolutionary and functional assessment of regulatory network motifs. *Genome Biol*, **6**(4), R35.

[33] Ingram, P. J., Stumpf, M. P. & Stark, J. (2006) Network motifs: structure does not determine function. *BMC Genomics*, **7**, 108.

[34] Payne, J. L. & Wagner, A. (2015) Function does not follow form in gene regulatory circuits. *Sci Rep*, **5**, 13015.

[35] Beber, M. E., Fretter, C., Jain, S., Sonnenschein, N., Müller-Hannemann, M. & Hütt, M.-T. (2012) Artefacts in statistical analyses of network motifs: general framework and application to metabolic networks. *J R Soc Interface*, **9**(77), 3426–3435.

[36] Ahnert, S. E. & Fink, T. (2016) Form and function in gene regulatory networks: the structure of network motifs determines fundamental properties of their dynamical state space. *J R Soc Interface*, **13**(120), 20160179.

[37] Lesk, A. M. & Konagurthu, A. S. (2020) Neighbourhoods in the yeast regulatory network in different physiological states. *Bioinformatics*. btaa831.

[38] Artzy-Randrup, Y., Fleishman, S. J., Ben-Tal, N. & Stone, L. (2004) Comment on “Network motifs: simple building blocks of complex networks” and “Superfamilies of evolved and designed networks”. *Science*, **305**(5687), 1107–1107.

[39] von Mering, C., Krause, R., Snel, B., Cornell, M., Oliver, S. G., Fields, S. & Bork, P. (2002) Comparative assessment of large-scale data sets of protein–protein interactions. *Nature*, **417**(6887), 399–403.

[40] Shin, C. J., Wong, S., Davis, M. J. & Ragan, M. A. (2009) Protein-protein interaction as a predictor of subcellular location. *BMC Syst Biol*, **3**, 28.

[41] Kumar, G. & Ranganathan, S. (2010) Network analysis of human protein location. *BMC Bioinformatics*, **11**(7), S9.

[42] Jazayeri, A. & Yang, C. C. (2020) Motif discovery algorithms in static and temporal networks: A survey. *J Complex Netw*, **8**(4). cnaa031.

[43] Byshkin, M., Stivala, A., Mira, A., Krause, R., Robins, G. & Lomi, A. (2016) Auxiliary Parameter MCMC for Exponential Random Graph Models. *J Stat Phys*, **165**(4), 740–754.

[44] Byshkin, M., Stivala, A., Mira, A., Robins, G. & Lomi, A. (2018) Fast maximum likelihood estimation via Equilibrium Expectation for large network data. *Sci Rep*, **8**, 11509.

[45] Borisenko, A., Byshkin, M. & Lomi, A. (2019) A simple algorithm for scalable Monte Carlo inference. *arXiv preprint arXiv:1901.00533v3*.

[46] Stivala, A., Robins, G. & Lomi, A. (2020) Exponential random graph model parameter estimation for very large directed networks. *PLoS One*, **15**(1), e0227804.

[47] Robins, G., Pattison, P., Kalish, Y. & Lusher, D. (2007) An introduction to exponential random graph (p^*) models for social networks. *Soc Networks*, **29**(2), 173–191.

[48] Lusher, D., Koskinen, J. & Robins, G., editors (2013) *Exponential Random Graph Models for Social Networks*. Structural Analysis in the Social Sciences. Cambridge University Press, New York.

[49] Amati, V., Lomi, A. & Mira, A. (2018) Social network modeling. *Annu Rev Stat Appl*, **5**, 343–369.

[50] Koskinen, J. (2020) Exponential Random Graph Modelling. In Atkinson, P., Delamont, S., Cernat, A., Sakshaug, J. & Williams, R., editors, *SAGE Research Methods Foundations*. SAGE, London.

[51] Cimini, G., Squartini, T., Saracco, F., Garlaschelli, D., Gabrielli, A. & Caldarelli, G. (2019) The statistical physics of real-world networks. *Nat Rev Phys*, **1**, 58–71.

[52] de Silva, E. & Stumpf, M. P. (2005) Complex networks and simple models in biology. *J R Soc Interface*, **2**(5), 419–430.

[53] Rolls, D. A., Wang, P., Jenkinson, R., Pattison, P. E., Robins, G. L., Sacks-Davis, R., Daraganova, G., Hellard, M. & McBryde, E. (2013) Modelling a disease-relevant contact network of people who inject drugs. *Soc Networks*, **35**(4), 699–710.

[54] Shalizi, C. R. & Rinaldo, A. (2013) Consistency under sampling of exponential random graph models. *Ann Stat*, **41**(2), 508–535.

[55] Schweinberger, M., Krivitsky, P. N., Butts, C. T. & Stewart, J. R. (2020) Exponential-family models of random graphs: inference in finite, super and infinite population scenarios. *Stat Sci*, **35**(4), 627–662.

[56] Rolls, D. A. & Robins, G. (2017) Minimum distance estimators of population size from snowball samples using conditional estimation and scaling of exponential random graph models. *Comput Stat Data An*, **116**, 32–48.

[57] Fronczak, P., Fronczak, A. & Bujok, M. (2013) Exponential random graph models for networks with community structure. *Phys Rev E*, **88**(3), 032810.

[58] Schweinberger, M. & Handcock, M. S. (2015) Local dependence in random graph models: characterization, properties and statistical inference. *J Am Stat Assoc*, **77**(3), 647–676.

[59] Schweinberger, M. & Luna, P. (2018) HERGM: Hierarchical exponential-family random graph models. *J Stat Softw*, **85**(1), 1–39.

[60] Wang, Y., Fang, H., Yang, D., Zhao, H. & Deng, M. (2019) Network clustering analysis using mixture exponential-family random graph models and its application in genetic interaction data. *IEEE/ACM Trans Comput Biol Bioinform*, **16**(5), 1743–1752.

[61] Babkin, S., Stewart, J., Long, X. & Schweinberger, M. (2020) Large-scale estimation of random graph models with local dependence. *Comput Stat Data An*, page 107029.

[62] Schweinberger, M. (2020) Consistent structure estimation of exponential-family random graph models with block structure. *Bernoulli*, **26**(2), 1205–1233.

[63] Handcock, M. S. & Gile, K. J. (2010) Modeling social networks from sampled data. *Ann Appl Stat*, **4**(1), 5–25.

[64] Pattison, P. E., Robins, G. L., Snijders, T. A. B. & Wang, P. (2013) Conditional estimation of exponential random graph models from snowball sampling designs. *J Math Psych*, **57**(6), 284–296.

[65] Stivala, A. D., Koskinen, J. H., Rolls, D., Wang, P. & Robins, G. L. (2016) Snowball sampling for estimating exponential random graph models for large networks. *Soc Networks*, **47**, 167–188.

[66] Robins, G., Pattison, P. & Woolcock, J. (2004) Missing data in networks: exponential random graph (p^*) models for networks with non-respondents. *Soc Networks*, **26**(3), 257–283.

[67] Koskinen, J. H., Robins, G. L., Wang, P. & Pattison, P. E. (2013) Bayesian analysis for partially observed network data, missing ties, attributes and actors. *Soc Networks*, **35**(4), 514–527.

[68] Desmarais, B. A. & Cranmer, S. J. (2012) Statistical inference for valued-edge networks: The generalized exponential random graph model. *PLoS One*, **7**(1), e30136.

[69] Krivitsky, P. N. (2012) Exponential-family random graph models for valued networks. *Electron J Stat*, **6**, 1100–1128.

[70] Krivitsky, P. N. & Handcock, M. S. (2014) A separable model for dynamic networks. *J R Stat Soc B Met*, **76**(1), 29–46.

[71] Pržulj, N. (2007) Biological network comparison using graphlet degree distribution. *Bioinformatics*, **23**(2), e177–e183.

[72] Yaveroğlu, O. N., Fitzhugh, S. M., Kurant, M., Markopoulou, A., Butts, C. T. & Pržulj, N. (2015) ergm.graphlets: A Package for ERG Modeling Based on Graphlet Statistics. *J Stat Softw*, **65**(12), 1–29.

[73] Hunter, D. R., Krivitsky, P. N. & Schweinberger, M. (2012) Computational statistical methods for social network models. *J Comput Graph Stat*, **21**(4), 856–882.

[74] Snijders, T. A. B. (2002) Markov chain Monte Carlo estimation of exponential random graph models. *Journal of Social Structure*, **3**(2), 1–40.

[75] Hunter, D. R. & Handcock, M. S. (2006) Inference in Curved Exponential Family Models for Networks. *J Comput Graph Stat*, **15**(3), 565–583.

[76] Hummel, R. M., Hunter, D. R. & Handcock, M. S. (2012) Improving Simulation-Based Algorithms for Fitting ERGMs. *J Comput Graph Stat*, **21**(4), 920–939.

[77] Krivitsky, P. N. (2017) Using contrastive divergence to seed Monte Carlo MLE for exponential-family random graph models. *Comput Stat Data An*, **107**, 149–161.

[78] Handcock, M. S., Hunter, D. R., Butts, C. T., Goodreau, S. M., Morris & Martina (2008) statnet: Software Tools for the Representation, Visualization, Analysis and Simulation of Network Data. *J Stat Softw*, **24**(1), 1–11.

[79] Morris, M., Handcock, M. & Hunter, D. (2008) Specification of exponential-family random graph models: Terms and computational aspects. *J Stat Softw*, **24**(4), 1–24.

[80] Hunter, D. R., Handcock, M. S., Butts, C. T., Goodreau, S. M. & Morris, M. (2008) ergm: A package to fit, simulate and diagnose exponential-family models for networks. *J Stat Softw*, **24**(3), 1–29.

[81] Wang, P., Robins, G. & Pattison, P. (2009) *PNet: program for the estimation and simulation of p^* exponential random graph models*. Department of Psychology, The University of Melbourne.

[82] Caimo, A. & Friel, N. (2011) Bayesian inference for exponential random graph models. *Soc Networks*, **33**(1), 41–55.

[83] Caimo, A. & Friel, N. (2014) Bergm: Bayesian Exponential Random Graphs in R. *J Stat Softw*, **61**(2), 1–25.

[84] Snijders, T. A. B., Pattison, P. E., Robins, G. L. & Handcock, M. S. (2006) New Specifications for Exponential Random Graph Models. *Sociol Methodol*, **36**(1), 99–153.

[85] Robins, G., Snijders, T. A. B., Wang, P., Handcock, M. & Pattison, P. (2007) Recent developments in exponential random graph (p^*) models for social networks. *Soc Networks*, **29**(2), 192–215.

[86] Salgado, H., Santos-Zavaleta, A., Gama-Castro, S., Millán-Zárate, D., Díaz-Peredo, E., Sánchez-Solano, F., Pérez-Rueda, E., Bonavides-Martínez, C. & Collado-Vides, J. (2001) RegulonDB (version 3.2): transcriptional regulation and operon organization in *Escherichia coli* K-12. *Nucleic Acids Res*, **29**(1), 72–74.

[87] Strauss, D. & Ikeda, M. (1990) Pseudolikelihood Estimation for Social Networks. *J Am Stat Assoc*, **85**(409), 204–212.

[88] van Duijn, M. A., Gile, K. J. & Handcock, M. S. (2009) A framework for the comparison of maximum pseudo-likelihood and maximum likelihood estimation of exponential family random graph models. *Soc Networks*, **31**(1), 52–62.

[89] Begum, M., Bagga, J. & Saha, S. (2014) Network motif identification and structure detection with exponential random graph models. *Network Biology*, **4**(4), 155–169.

[90] Bulashevska, S., Bulashevska, A. & Eils, R. (2010) Bayesian statistical modelling of human protein interaction network incorporating protein disorder information. *BMC Bioinformatics*, **11**(1), 46.

[91] Azad, A., Lawen, A. & Keith, J. M. (2017) Bayesian model of signal rewiring reveals mechanisms of gene dysregulation in acquired drug resistance in breast cancer. *PLoS One*, **12**(3), e0173331.

[92] Schuldiner, M., Collins, S. R., Thompson, N. J., Denic, V., Bhamidipati, A., Punna, T., Ihmels, J., Andrews, B., Boone, C., Greenblatt, J. F. et al. (2005) Exploration of the function and organization of the yeast early secretory pathway through an epistatic miniaarray profile. *Cell*, **123**(3), 507–519.

[93] Simpson, S. L., Hayasaka, S. & Laurienti, P. J. (2011) Exponential random graph modeling for complex brain networks. *PLoS One*, **6**(5), e20039.

[94] Simpson, S. L., Moussa, M. N. & Laurienti, P. J. (2012) An exponential random graph modeling approach to creating group-based representative whole-brain connectivity networks. *Neuroimage*, **60**(2), 1117–1126.

[95] Sinke, M. R., Dijkhuizen, R. M., Caimo, A., Stam, C. J. & Otte, W. M. (2016) Bayesian exponential random graph modeling of whole-brain structural networks across lifespan. *Neuroimage*, **135**, 79–91.

[96] Obando, C. & De Vico Fallani, F. (2017) A statistical model for brain networks inferred from large-scale electrophysiological signals. *J R Soc Interface*, **14**(128), 20160940.

[97] Stillman, P. E., Wilson, J. D., Denny, M. J., Desmarais, B. A., Bhamidi, S., Cranmer, S. J. & Lu, Z.-L. (2017) Statistical modeling of the default mode brain network reveals a segregated highway structure. *Sci Rep*, **7**(1), 11694.

[98] Grazioli, G., Martin, R. W. & Butts, C. T. (2019a) Comparative Exploratory Analysis of Intrinsically Disordered Protein Dynamics Using Machine Learning and Network Analytic Methods. *Front Mol Biosci*, **6**, 42.

[99] Grazioli, G., Yu, Y., Unhelkar, M. H., Martin, R. W. & Butts, C. T. (2019b) Network-based classification and modeling of amyloid fibrils. *J Phys Chem B*, **123**(26), 5452–5462.

[100] Mewes, H.-W., Frishman, D., Güldener, U., Mannhaupt, G., Mayer, K., Mokrejs, M., Morgenstern, B., Münsterkötter, M., Rudd, S. & Weil, B. (2002) MIPS: a database for genomes and protein sequences. *Nucleic Acids Res*, **30**(1), 31–34.

[101] Ruepp, A., Zollner, A., Maier, D., Albermann, K., Hani, J., Mokrejs, M., Tetko, I., Güldener, U., Mannhaupt, G., Münsterkötter, M. et al. (2004) The FunCat, a functional annotation scheme for systematic classification of proteins from whole genomes. *Nucleic Acids Res*, **32**(18), 5539–5545.

[102] Handcock, M. S., Hunter, D. R., Butts, C. T., Goodreau, S. M., Krivitsky, P. N., Bender-deMoll, S. & Morris, M. (2016) *statnet: Software Tools for the Statistical Analysis of Network Data*. The Statnet Project (<http://www.statnet.org>). R package version 2016.9.

[103] Costanzo, M. C., Crawford, M. E., Hirschman, J. E., Kranz, J. E., Olsen, P., Robertson, L. S., Skrzypek, M. S., Braun, B. R., Hopkins, K. L., Kondu, P., Lengieza, C., Lew-Smith, J. E., Tillberg, M. & Garrels, J. I. (2001) YPDTM, PombePDTM and WormPDTM: model organism volumes of the BioKnowledgeTM Library, an integrated resource for protein information. *Nucleic Acids Res*, **29**(1), 75–79.

[104] Clauset, A., Shalizi, C. R. & Newman, M. E. (2009) Power-law distributions in empirical data. *SIAM Rev*, **51**(4), 661–703.

[105] Gillespie, C. S. (2015) Fitting Heavy Tailed Distributions: The poweRlaw Package. *J Stat Softw*, **64**(2).

[106] Robins, G., Pattison, P. & Wang, P. (2009) Closure, connectivity and degree distributions: Exponential random graph (p^*) models for directed social networks. *Soc Networks*, **31**(2), 105–117.

[107] Koskinen, J. & Daraganova, G. (2013) Exponential random graph model fundamentals. In Lusher, D., Koskinen, J. & Robins, G., editors, *Exponential Random Graph Models for Social Networks*, chapter 6, pages 49–76. Cambridge University Press, New York.

[108] Hunter, D. R. (2007) Curved exponential family models for social networks. *Soc Networks*, **29**(2), 216–230.

[109] Cantwell, G. T., Liu, Y., Maier, B. F., Schwarze, A. C., Serván, C. A., Snyder, J. & St-Onge, G. (2020) Thresholding normally distributed data creates complex networks. *Phys Rev E*, **101**(6), 062302.